http://journal.uir.ac.id/index.php/JGEET

E-ISSN : 2541-5794
P-ISSN : 2503-216X

Journal of Geoscience,
Engineering, Environment, and Technology
Vol 9 No 1 2024

RESEARCH ARTICLE

Geochemistry of Igneous Rocks of Citirem Formation and Its Implications for the Tectonic Setting in Ciletuh – Palabuhanratu UNESCO Global Geopark Area

Hafidhah Nurul Haq[1,*], Mega F. Rosana[1], Cipta Endyana[1], Katon S. A. Nugraha.[1], Irpan Alamsyah[1]

[1]*Faculty of Geological Engineering, Petrology and Mineralogy, Padjadjaran University, Jl. Dipati Ukur No. 35, Bandung, Indonesia*

* Corresponding author : hafidhah11001@mail.unpad.ac.id
Tel.:+6285940387170
Received: Sep 18, 2023; Accepted: Mar 7, 2024.
DOI: 10.25299/jgeet.2024.9.1.14367

Abstract

The igneous rocks of the Citirem Formation in the Ciletuh – Palabuhanratu UNESCO Global Geopark area petrographically not only consist of basalt, but also andesite, dacite, and gabbro. The characteristics of basalts Citirem Formation are composed of plagioclase 43% – 58% and olivine, mostly have amygdaloidal and aphanitic textures. Andesites are composed of 45% – 65% plagioclase, absence of olivine, mostly aphanitic and trachytic, some have intergranular textures. Dacite comprises 50% plagioclase, 20% quartz, and the absence of olivine, and aphanitic, intersertal textures. Gabbros are composed of 62% plagioclase, 6% – 12% olivine, with phaneritic texture. Based on the plot of the major elements vs SiO_2 diagram, MgO, FeOt (Fe_2O_3+FeO), CaO, and TiO_2 show a negative correlation with SiO_2. In comparison, Na_2O and K_2O show a positive correlation with SiO_2. The lithology of igneous rocks of Citirem Formation are basalt, trachybasalt, basaltic trachyandesite, trachyandesite, andesite, dacite and gabbro based on a plot of the Na_2O+K_2O vs SiO_2 diagram for volcanic and plutonic rocks. The origin of magma type can be distinguished based on the plot of K_2O vs SiO_2 diagrams, the igneous rocks of Citirem Formation are divided into low-K, medium-K, high-K, and shoshonite magma series. Dacite STA 2, andesite STA 7, basaltic andesite STA 8, trachyandesite STA 10 and gabbro STA 14 are calc-alkaline based on triangular diagram Th-Hf-Ta-Zr-Nb. Gabbro STA 17 indicates IAT (island arc tholeiite), trachybasalt STA 19, basalt STA 20 and basaltic trachyandesite STA 27 are E-MORB, WPT (within plate tholeiitic), In contrast, trachybasalt STA 28 is WPA (within plate alkali). Primitive mantle long, NMORB-normalized REE patterns and chondrites-normalized show some rocks have distinctive patterns that have similarities with suprasubduction zone ophiolite rocks, MORB of Mirdita ophiolite, and some show similarities with patterns from OIB and E-MORB.

Keywords: igneous rocks, suprasubduction zone, MORB, Citirem

1. Introduction

The Ciletuh – Palabuhanratu UNESCO Global Geopark area is fascinating to study because there are a variety of mixed rocks resulting from collisions between the Eurasian and Indo-Australian plates, these rocks consist of oceanic bedrock to the edge of the continent, such as basic to ultra-basic igneous rocks (relatives of ophiolites), metamorphic rocks, deep-sea sedimentary rocks, and groups of continental sedimentary rocks (Rosana, 2006). These various types of rocks are the oldest group of rocks (ranging from 120-65 million years ago) exposed on the island of Java (Schiller, 1991), named mélange because they are mixed (Suhaeli, et al., 1977) or olistostroms (Sartono and Murwanto, 1987).

The Citirem Formation belongs to the Pre-Tertiary rock group. So far, the presence of the Citirem Formation is considered a mélange and is included in the oldest formation in West Java. The Pre-Tertiary group consists of mélange rocks, a mixture of metamorphic, alkaline, ultra-alkaline rocks and the Citirem Formation. Meanwhile, the Tertiary rock group consists of the Ciletuh Formation, Bayah Formation and Jampang Formation. Geochemical research is carried out in the research area because it has not been widely used to identify the characteristics of rocks and determine their tectonic environment (Sukamto, 1975).

The Citirem complex can be grouped into three rock units and coastal alluvium and deposits. The ages from old to younger are: (1) Basalt Lava units, also referred to as the Citirem Formation (Sukamto, 1975), are of Pre-Tertiary age; (2) Quartz Sandstone Unit, also called Ciletuh Formation (Sukamto, 1975), is of Late Eocene – Early Oligocene age; and (3) Limestone Units the Cibodas Formation (Sukamto, 1975) of Upper Miocene age and Quaternary Coastal Alluvium Deposits.

Sukamto (1975) in his statement explained that the age of basalt lava (Citirem Formation) and peridotite-serpentinite (Gunung Beas Formation) is relatively the same because these rocks are relatives of ophiolites. Therefore, peridotite-serpentinite and basalt lava likely formed on the Indo-Australian plate. Along with the collision between plates, metamorphic rocks were formed in the Late Cretaceous, namely the schist of the Pasir Luhur Formation.

Based on these geological phenomena, the Citirem area is fascinating to study and can be used as a place to study the concept of plate tectonics. The research was conducted

to obtain geochemical data on igneous rocks in the Citirem area, to interpret the tectonic setting.

2. Research Area

The research area is located in Citirem and its surroundings in the Ciletuh – Palabuhanratu UNESCO Global Geopark area, bounded by coordinates between 106° 21' 55.94" - 106° 25' 6.14" E and 7° 15' 48.21" – 7° 19' 23.93" S. Administratively, the location of this research is located within the government area of Ciemas Sub-district, Sukabumi Regency, West Java Province (Fig.1). Geologically, the research area is included in the Basalt Lava Unit, also referred to as the Pre-Tertiary Citirem Formation (Sukamto, 1975) (Fig.2).

Fig 1. Research area in Ciletuh-Palabuhanratu UNESCO Global Geopark Area

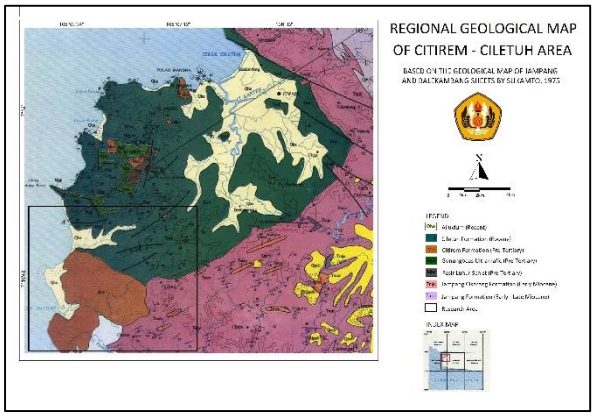

Fig 2. Geological Map of the Research Area, Citirem Formation symbolized by Mcv (Sukamto, 1975).

3. Methods

The method used in this study started from the field observation stage, and rock samples were taken around the coast of Cikepuh and Citirem areas, Ciemas Sub-District, Sukabumi, West Java. Followed by petrographic analysis at the Petrology and Mineralogy Laboratory, Faculty of Geological Engineering, Padjadjaran University. Analysis of the major elements of rock chemistry based on XRF (X-ray Fluorescence) data. Trace elements and Rare Earth Elements (REE) were analyzed based on Inductive Couple Plasma Emission Mass Spectrometry (ICP-MS) measurement results. The chemical analysis was carried out at Intertek Laboratory Jakarta. Geochemical data is processed and analyzed through a multi-diagram approach. The results of the petrograph and the output of various diagrams are combined for the interpretation of its tectonic settings.

4. Results

4.1 Distribution and Location of Rock Sampling

Random sampling of rock samples is carried out locally depending on the presence of outcrops to obtain an overview of geological conditions. From 30 observation stations, 19 igneous rock samples were found and sampled (Fig. 3), ten of which were then chemically analyzed, namely STA 2, STA 7, STA 8, STA 10, STA 14, STA 17, STA 19, STA 20, STA 27 and STA 28. The observation locations were around Legon Mata Hiang, Batu Kereta, Alor Buntu, Alor Panganten, Pamoek, Cikahuripan, Pulo Keris, Cibanteng, Cibuaya River and Leuwi Cangkring Cipanarikan River.

4.2 Citirem Formation Lithology

Based on the results of petrographic analysis (megascopic and microscopic minerals), the igneous rocks of the Citirem Formation in the study area consist of several lithologies: basalt, gabbro, dacite, and andesite. A summary of petrographic data is presented in Table 1.

4.2.1 Basalt

Basalts (STA 16, 19, 20, 22, 27, 28, 29, 30) were exposed with varying thicknesses (~5 meters to >10 meters) in several places, in Alor Panganten (STA 16), Cibuaya River (STA 19 and 20), the mouth of the Citirem River (STA 22) and Leuwi Cangkring Cipanarikan River (STA 27, 28, 29, 30). The rock outcrop shows a pillow structure (Fig. 4) with a weathered black color and a fresh dark gray color.

Microscopically, basalt (STA 27) has aphanitic, intersertal and amygdaloidal textures, vesicular are filled with chlorite. The ground mass is composed of plagioclase microliths and glass. The common phenocrysts are plagioclase, olivine, pyroxene and opaque minerals. Some mafic mineral phenocrysts are altered into chlorite.

Fig. 4. A: basalt outcrops on the walls and floors of the Cipanarikan River (STA 27), B: basalt outcrops (STA 27) show globular-shaped pillow lava structures in the Leuwi Cangkring, Cipanarikan River. Photomicrograph of basalt STA 16 (4x magnification, scale: 500 µm) is showed in C: parallel polarizers, D: crossed polarizers, showing the aphanitic, intersertal and amygdaloidal textures of basalt lava. There are phenocrysts of mafic minerals that are altered to chlorite.

4.2.2 Gabbro

Gabbro is represented by STA 14 and 17, exposed on the Pulo Keris and Cibanteng coastal cliffs with varying thicknesses (~5 meters to >10 meters). Megascopically, it

generally has a fresh color of black, mesocratic to melanocratic (Fig. 5).

Microscopically, the characteristic rock (STA 14) is greenish-gray, has a phaneritic, intergranular, holocrystalline, subhedral, hypidiomorphic texture. The common mineral assemblages present in rocks are plagioclase in large sizes, olivine, pyroxene, orthoclase and opaque minerals. Opaque mineral inclusions are present in pyroxene and plagioclase minerals.

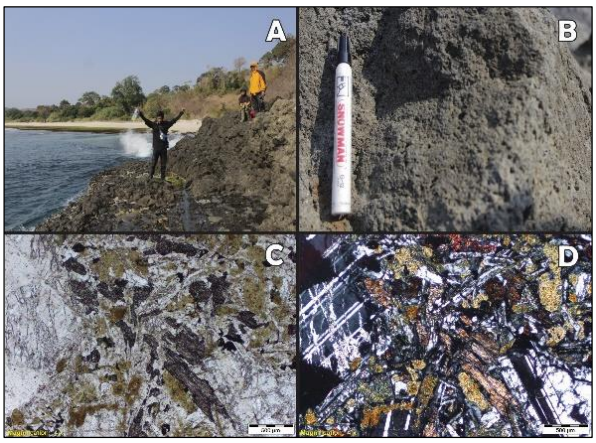

Fig.5. A: gabbro outcrop (STA 14) on the coastal cliff and B: close view gabbro outcrop (STA 14) in the Pulo Keris area. Photomicrograph of gabbro STA 14 (4x magnification, scale: 500 µm) is showed in C: parallel polarizers, D: crossed polarizers with phaneritic, intergranular, plagioclase, pyroxene, olivine phenocrysts.

4.2.3 Dacite

Dacite STA 2 was exposed with a thickness of ~3 meters around Legon Mata Hiang with a light gray color and vesicular structure (Fig. 6A and 6B).

Microscopically, the texture of dacite (Fig. 5 C and 5D) is aphanitic, intersertal, equigranular, hypocrystalline, subhedral to anhedral, generally hypidiomorphic. The ground mass is mostly plagioclase microliths, feldspar and glass. It comprises plagioclase, quartz, orthoclase, pyroxene, opaque minerals. It appears that plagioclase is altered.

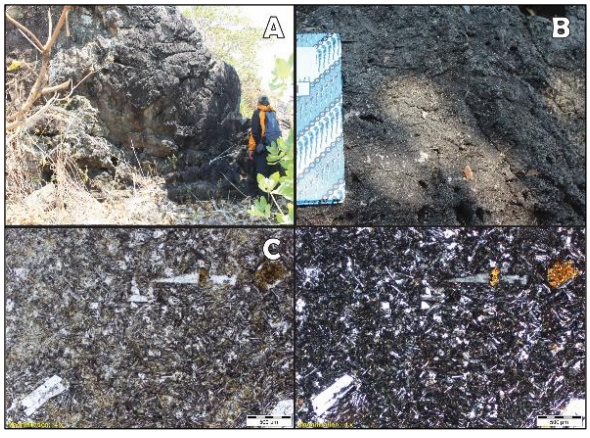

Fig. 6. Dacite outcrop of STA 2, A: distant view, B: close view in Legon Mata Hiang are. Photomicrograph of dacite STA 2 (4x magnification, scale: 500 µm) is showed in C: parallel polarizers and D: crossed polarizers with intersertal texture, showing plagioclase, quartz and pyroxene as phenocryst.

4.2.4 Andesite

Andesite outcrops (STA 1, 4, 6, 7, 8, 9, 10, 11, 14) were found in situ and large blocks with a diameter around > 2 – 10 meters in Legon Mata Hiang, Batu Kereta, Alor Buntu, Pamoek, Cikahuripan. Megascopically, it has a characteristic brownish-black weathered color, gray fresh color, aphanitic texture, and mesocratic color index (Fig. 7).

Microscopically, andesite has a trachytic texture, with hypocrystalline degree of crystallization. The groundmass is composed of plagioclase microliths, feldspar and glass. Phenocrysts are plagioclase, k-feldspar, pyroxene, opaque minerals, and quartz.

Fig. 7. Andesite outcrops of STA 10, A: distant view and B: close view in Cikahuripan. Andesite photomicrograph STA 10 (4x magnification, scale: 500 µm) is showed in C: parallel polarizers and D: crossed polarizers showing aphanitic, trachytic texture.

4.3 Geochemical Characteristics of Igneous Rocks of The Citirem Formation

Ten representative rock samples were selected for geochemical analysis using XRF and ICP-MS methods. The results of XRF 10 samples of research rocks and some comparison rocks from Mirdita Ophiolite (Dilek, 2008) can be viewed in Table 2. Six samples of research rocks have a loss on ignition (LOI) below 4%. This data informs that six rock samples are relatively fresh and do not exceed the threshold, making them suitable for chemical analysis of rocks. The other four have LOIs >4% - <6%, therefore, caution is needed in analyzing them.

4.3.1 Geochemistry of Major Elements

The XRF method analyzes the major elements of 10 representative rock samples. After obtaining data on the content of the major elements, analysis of various diagrams is carried out by plotting according to the parameters used.

The results of geochemical analysis of the major elements in rock samples are, SiO_2 content 46.20 - 64.72 wt%, Al_2O_3 15.13 - 18.25 wt%, CaO 4.66 - 8.67 wt%, Fe_2O_3 4.34 - 9.07 wt%, K_2O 0.4 - 2.22 wt%, MgO 1.34 - 9.45 wt%, Na_2O 2.52 - 5 wt%, TiO_2 0.92 - 1.83 wt%, P_2O_5 0.159 - 0.440 wt%. In the results of the analysis, it can be seen that SiO_2, Al_2O_3, CaO, FeOt, MgO, and TiO_2 have medium to quite high content. The high level of the major elements forming the rock is characteristic of the minerals plagioclase ($[Ca,Na]AlSi_3O_8$), pyroxene ($[Ca,Na][Mg,Fe,Al][Si,Al]_2O_6$), and olivine ($[Mg,Fe]_2SiO_4$).

Diagrams of the major elements against SiO_2 are used to determine the magma evolution (Harker, 1909 in Rollinson, 1993). An irregular and scattered plot distribution is sometimes found in variation diagrams.

Table 1. Summary of lithology of igneous rocks of the Citirem Formation (research) based on petrographic analysis

Site	Location	Texture	Mineralogy Composition						Lithology (Streckeisen, 1976, 1978)
			Plg	Ol	Px	Qtz	KF	Opq	
STA 1	Legon Mata Hiang	Aphanitic, intergranular	50%		17%	8%	5%	3%	Andesite
STA 2	Legon Mata Hiang	Aphanitic, intersertal	50%	-	8%	20%	7%	5%	Dacite
STA 4	Legon Mata Hiang	Aphanitic, trachytic	65%	-	10%	5%	4%	7%	Andesite
STA 6	Batu Kereta	Aphanitic	40%	-	8%	25%	10%	3%	Andesite
STA 7	Alor Buntu	Aphanitic, trachytic, intergranular	55%	-	15%	9%	4%	4%	Andesite
STA 8	Pamoek	Aphanitic, trachytic, intergranular	60%	-	18%	3%	3%	5%	Andesite
STA 9	Cikahuripan	Aphanitic	55%	-	13%	6%	3%	5%	Andesite
STA 10	Cikahuripan	Aphanitic, trachytic	55%	-	8%	8%	13%	3%	Andesite
STA 11	Cikahuripan	Aphanitic, intersertal	45%	-	14%	10%	7%	8%	Andesite
STA 14	Pulo Keris	Phaneritic, intergranular	62%	12%	8%	-	2%	5%	Gabbro
STA 16	Alor Panganten	Aphanitic, amygdaloidal	57%	4%	15%	3%	5%	7%	Basalt
STA 17	Cibanteng	Phaneritic	62%	6%	18%	-	2%	5%	Gabbro
STA 19	Cibuaya River	Aphanitic	59%	18%	3%	-	5%	6%	Basalt
STA 20	Cibuaya River	Aphanitic	50%	10%	16%	-	8%	6%	Basalt
STA 22	Mouth of Citirem River	Porphyritic, amygdaloidal	50%	-	3%	4%	5%	5%	Basalt
STA 27	Leuwi Cangkring Cipanarikan River	Porphyritic, amygdaloidal	58%	15%	6%	-	7%	5%	Basalt
STA 28	Leuwi Cangkring Cipanarikan River	Aphanitic, amygdaloidal	49%	15%	10%	-	9%	7%	Basalt
STA 29	Cipanarikan River	Aphanitic, intergranular, amygdaloidal	45%	10%	3%	5%	7%	5%	Basalt
STA 30	Cipanarikan River	Porphyritic, amygdaloidal	43%	3%	10%	3%	5%	5%	Basalt

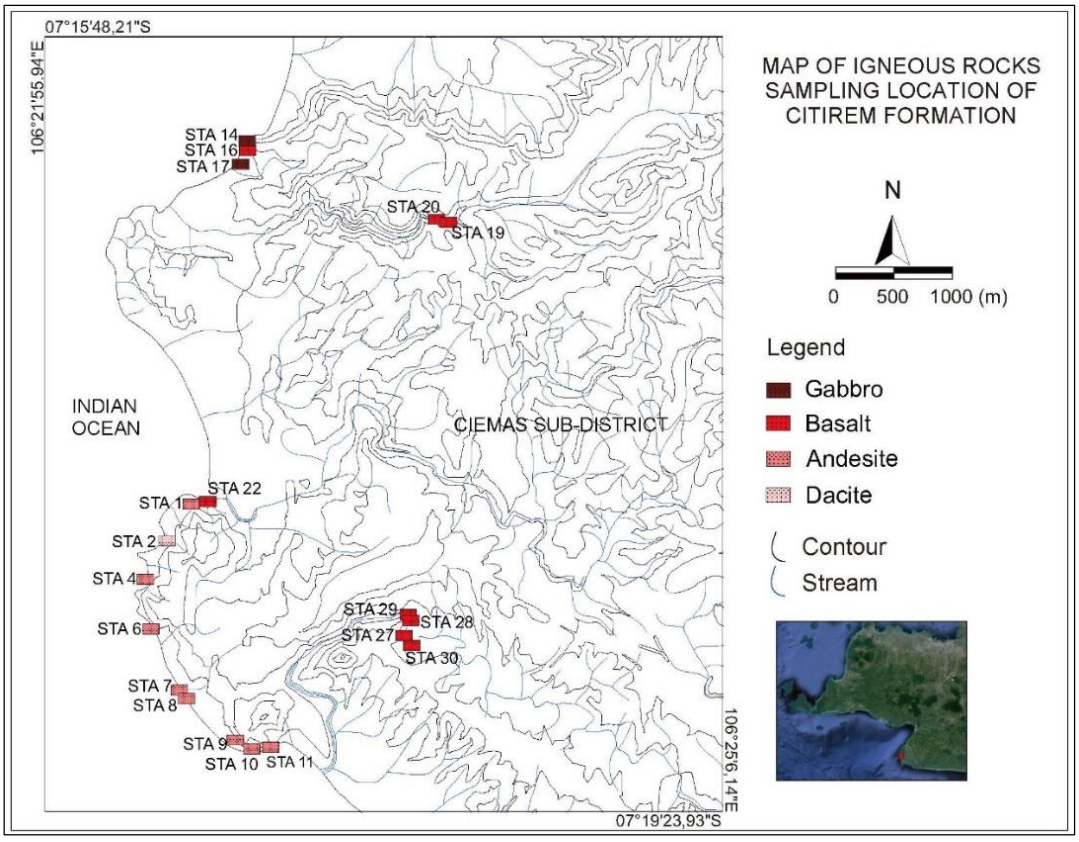

Fig. 3. Map of Igneous Rocks Sampling Location of Citirem Formation, Ciletuh – Palabuhanratu UNESCO Global Geopark.

Table 2. The result of the analysis of the major elements content (wt.%) of the Citirem Formation rock samples and its lithology based on Middlemost (1994) for volcanic rocks and Cox, et al. (1979) for plutonic rocks. Rocks from Mirdita Ophiolite (Dilek, 2008) as a comparison.

Site	SiO_2	Al_2O_3	CaO	Fe_2O_3	K_2O	MgO	MnO	Na_2O	P_2O5	TiO_2	LOI	Lithology
STA-2	64,72	15,45	4,66	4,62	2,22	1,80	0,09	4,12	0,302	0,92	0,793	Dacite
STA-7	56,59	15,90	8,28	6,28	0,70	3,19	0,09	4,36	0,430	1,14	2,259	Andesite
STA-8	54,59	17,50	7,86	6,48	0,62	4,78	0,09	4,43	0,423	1,29	0,906	Basaltic Andesite
STA-10	60,57	16,08	5,69	4,34	2,62	1,34	0,13	4,84	0,440	1,23	2,097	Trachyandesite
STA-14	49,71	17,19	6,91	8,10	0,47	6,97	0,14	5,00	0,186	1,29	3,775	Gabbro
STA-17	48,96	18,25	8,67	7,88	0,40	7,49	0,13	3,43	0,159	1,16	2,693	Gabbro
STA-19	46,75	16,76	6,06	8,77	0,97	8,60	0,14	4,01	0,315	1,37	5,412	Trachybasalt
STA-20	46,20	15,95	7,55	8,92	1,51	9,45	0,20	2,52	0,346	1,63	4,802	Basalt
STA-27	48,79	16,81	6,42	7,66	1,21	7,51	0,22	4,53	0,324	1,29	4,807	Basaltic trachyandesite
STA-28	46,89	15,13	7,09	9,07	1,76	8,05	0,19	3,58	0,389	1,83	5,253	Trachybasalt
Mirdita Ophiolite 72-Al-01	64,64	12,86	1,61	6,85	0,13	4,05	0,08	4,46	0,05	0,52	3,66	Dacite lava
EMP Mirdita O. 17-Al-00	53,20	15,51	6,34	11,10	0,23	5,99	0,18	3,81	0,05	0,68	2,55	Basaltic andesite lava
EMP Mirdita O. 25-Al-00	60,1	14,22	4,37	9,64	0,13	4,18	0,17	3,83	0,04	0,57	2,95	Andesite lava
West Part Mirdita O. 35-Al-00	49,92	13,16	9,61	14,37	0,04	5,45	0,21	3,03	0,17	2,24	2,26	Basalt *dike*
WSP Mirdita O. 98-Al-01	48,99	17,55	12,44	8,07	0,48	7,13	0,17	3,04	0,02	0,66	1,69	Basalt *pillow* lava
WMP Mirdita O. 62a-Al-01	47,44	14,04	9,91	10,27	0,06	6,61	0,21	2,04	0,21	1,76	4,24	Basalt *pillow* lava

Table 3. Normative Mineral Percentage of Igneous Rocks of Citirem Formation

Mineral	STA 2	STA 7	STA 8	STA 10	STA 14	STA 17	STA 19	STA 20	STA 27	STA 28
Quartz	20,06	9,06	4,13	10,9	0	0	0	0	0	0
Anorthite	17,168	21,82	26,316	14,511	23,119	33,493	25,084	28,012	22,061	20,151
Albite	34,947	37,062	37,824	41,124	40,662	29,277	34,185	21,493	36,384	29,019
Orthoclase	13,18	4,14	3,72	15,54	2,78	2,36	5,79	8,98	7,15	10,46
Nepheline	0	0	0	0	0,98	0	0	0	1,15	0,83
Diopside	3,29	13,44	8,22	8,97	8,02	7,05	2,5	5,95	6,21	10,15
Hypersthene	5,76	5,47	12,07	1,15	0	12,31	0,69	11,62	0	0
Olivine	0,00	0	0	0	13,69	6,21	18,43	9,91	15,09	15,02
Ilmenite	1,75	2,17	2,47	2,36	2,45	2,22	2,62	3,11	2,47	3,49
Magnetite	2,02	2,74	2,86	1,9	3,54	3,45	3,84	3,32	3,35	3,97
Apatite	0,70	1	1	1,02	0,44	0,37	0,74	0,81	0,76	0,9
Lithology (Middlemost, 1994)	Dacite	Andesite	Basaltic Andesite	Trachy-andesite	Gabbro	Gabbro	Trachy-basalt	Basalt	Basaltic Trachy-andesite	Trachy-basalt

Table 4. The result of the analysis of the rare earth elements content of the Citirem Formation rock samples (in ppm) following comparisons of Ophiolite rocks Mirdita, Albania (Dilek, 2008) and E-type MORB & OIB (Sun &; McDonough, 1989)

Site	La	Ce	Pr	Nd	Sm	Eu	Gd	Tb	Dy	Ho	Er	Tm	Yb	Lu	Lithology
STA-2	13,1	31,3	3,89	16,1	4	1	4,2	0,69	4,4	0,9	2,4	0,4	2,6	0,45	Dacite
STA-7	10	26,3	3,5	15,9	4,2	1,2	4,5	0,72	4,8	0,9	2,6	0,4	2,6	0,43	Andesite
STA-8	10,8	28,8	3,89	17,7	4,5	1,3	5	0,81	5,3	1,1	2,9	0,4	2,9	0,48	Basaltic Andesite
STA-10	16,6	41,1	5,15	22,1	5,1	1,4	5,7	0,88	5,8	1,1	3,1	0,4	3	0,48	Trachy Andesite
STA-14	6	16,8	2,41	12,5	3,2	1,1	4	0,65	4,4	0,9	2,4	0,3	2,4	0,36	Gabbro
STA-17	4,7	13,2	2,06	9,2	2,7	1	3,1	0,52	3,4	0,7	1,8	0,3	1,8	0,29	Gabbro
STA-19	10,4	23,8	2,95	13,5	3,5	1,1	3,9	0,72	4,6	0,9	2,6	0,4	2,7	0,42	Trachybasalt
STA-20	12,4	27,7	3,42	15,5	3,8	1,2	4,2	0,68	4,1	0,8	2,3	0,3	2,2	0,34	Basalt
STA-27	12,3	28,4	3,57	15,6	3,6	1,1	4,1	0,64	4	0,8	2,1	0,3	2,1	0,32	Basaltic Trachyandesite
STA-28	16,1	34,8	4,17	18,4	4,4	1,4	4,8	0,75	4,6	0,9	2,2	0,3	2,2	0,33	Trachybasalt
West Part Mirdita O. 35-Al-00	3,39	11,5	2,10	12,45	5,34	2	7,49	1,47	9,79	2,13	5,9	0,86	5,34	0,82	Basalt dike
WMP Mirdita O. 62a-Al-01	4	12,83	2,25	13,36	5,51	1,76	7,78	1,49	10,14	2,13	6,11	0,89	5,57	0,,88	Basalt pillow lava
E-Type MORB	6,3	15	2,05	9	2,6	0,91	2,97	0,53	3,55	0,79	2,31	0,356	2,37	0,354	Basalt
OIB	37	80	9,7	38,5	10	3	7,62	1,05	5,6	1,06	2,62	0,35	2,16	0,3	Basalt

Table 5. The result of the analysis of the trace element content of Citirem Formation rock samples (in ppm) following comparisons of Mirdita Ophiolite rocks (Dilek, 2008) and E-type MORB &; OIB (Sun &; McDonough, 1989).

Site	Cr	Co	Ni	Pb	Ba	Rb	Sr	V	W	Th	U	Nb	Ta	Zr	Hf	Sb	Li	Y	Lithology
STA-2	29	10	19	6	127	59,7	166	89	0,5	4,39	1,64	8	0,62	222	5,5	0,2	27,4	25,8	Dacite
STA-7	65	22	41	3	59	13,6	207	123	0,4	1,74	1,14	6,3	0,55	173	4,2	0,2	14	27,1	Andesite
STA-8	65	21	41	3	61	7,7	233	139	0,2	1,99	0,73	7,3	0,59	193	4,6	<0.1	10,3	29,9	Basaltic Andesite
STA-10	6	13	9	4	179	52,3	199	114	0,7	4,1	2,96	13,9	0,98	244	5,8	0,2	15,4	32	Trachyandesite
STA-14	146	33	80	2	54	6,1	219	157	0,2	1,19	0,28	3,8	0,32	118	3,2	<0.1	12,3	23,6	Gabbro
STA-17	222	32	95	1	40	3,4	258	138	0,3	0,63	0,35	3,3	0,24	74,9	2,2	<0.1	11,9	19,2	Gabbro
STA-19	112	34	98	1	178	9,3	238	156	0,2	1,77	0,37	14,7	0,99	123	3,1	<0.1	13,7	25,6	Trachybasalt
STA-20	153	37	157	1	258	16,7	574	158	0,2	2,05	0,63	19,4	1,27	132	3,3	0,2	13,7	23,4	Basalt
STA-27	133	31	117	2	214	22,9	333	144	0,2	2,47	0,53	16,2	1,1	130	3,2	<0.1	16,5	21,7	Basaltic Trachy Andesite
STA-28	164	36	112	2	235	31,6	221	165	0,4	2,8	0,73	29,2	1,91	139	3,6	<0.1	21,2	23,1	Trachybasalt
EMP Mirdita O. 17-Al-00	42	55	31				106	276						45				19	And. Bas. Lava
EMP Mirdita O. 25-Al-00	30	49	18				85	305						44				19	Andesite lava
West Part Mirdita O. 35-Al-00	66	61	42	0,21		3	73	339		0,15	0,05		0,11	150	3,78			59	Basalt dike
WSP Mirdita O. 98-Al-01	335	49	132			10	240	293						31				24	Basalt pl.lava
WMP Mirdita O. 62a-Al-01	381	48	109	0,34	3	2	74	293		0,15	0,07		0,13	168	4,01			64	Basalt pl.lava
E-type MORB				0,6	57	5,04	155		0,092	0,6	0,18	8,3	0,47	73	2,03	0,01	3,5	22	Basalt
OIB				3,2	350	31	660		0,56	4	1,02	48	2,7	280	7,80	0,03	5,6	29	Basalt

This is partly due to the rock samples showing porphyritic texture or due to the accumulation of certain minerals (Hutabarat, 2006). The diagrams will show the positive or negative correlation of the content of the major elements oxide to SiO_2. Based on the plots on the Harker diagram shown in fig. 8, the rock sample shows a negative correlation of MgO, FeOt (Fe_2O_3 + FeO), CaO, TiO_2, to SiO_2. That is, MgO, FeOt, CaO, TiO_2 decrease in levels along with the increase in SiO_2. While Na_2O and K_2O show a positive correlation with SiO_2, where Na_2O and K_2O increase levels as SiO_2 levels increase.

The negative correlation of MgO, FeO_t, TiO_2 to SiO_2 is a manifestation that the normal crystallization process of the minerals olivine ($[Mg,Fe]_2SiO_4$) and then the pyroxene ($[Mg,Fe,Ca,Na][Mg,Fe,Al]Si_2O_6$) will decrease. The positive correlation of Na_2O and K_2O to SiO_2 indicates the presence of a normal feldspar crystallization process. This results in the formation of orthoclase ($KAlSi_3O_8$) and albite ($Na[AlSi_3O_8]$. This pattern supports petrographic analysis showing that large quartz is accompanied by the presence of orthoclase and albit as in STA 2, 7, 8, 10. Meanwhile, the absence of quartz is accompanied by the presence of olivine and pyroxene as in STA 14, 17, 19, 20, 27.

Al_2O_3 and CaO initially showed increased levels up to 55% SiO_2 values, but at SiO_2 values above 55%, Al_2O_3 and CaO levels decreased. While in P_2O_5, a decrease in levels occurs when the SiO_2 value is above 60%.

The chemical variations and deflection point trends in indicates a relationship of changes in mineral assemblages and mineral chemistry. The bending of the correlation lines reflects that fractional crystals result from chemical variations in the magma. The likely result of contamination and crustal melts is the presence of Al_2O_3 and MgO, which vary extremely. In table 2, the MgO content shows a fairly extreme variation of 1.34 – 9.45 wt. %. Meanwhile, a decrease in P_2O_5 levels accompanied by a reduction in MgO levels indicates a variation in levels of fractional crystallization or partial melting (Hutabarat, 2006).

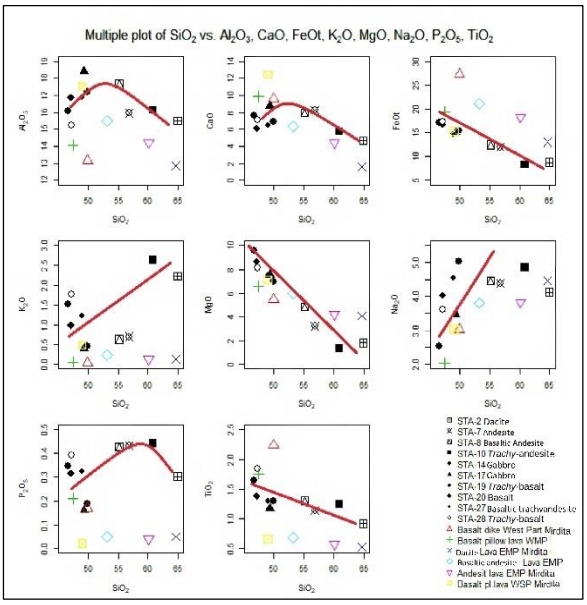

Fig. 8. The plots of the Citirem Formation rock sample on the Harker Diagram show a negative correlation of MgO, FeO_t (Fe_2O_3+FeO), TiO_2 to SiO_2. While Na_2O and K_2O show a positive correlation with SiO_2. Al_2O_3, CaO and P_2O_5 showed a change in trend (deflection occurs), initially positive to negative for SiO_2 (the example of the research rock is symbolized by black).

The value of the major elemental oxides can be used to determine the normative value of minerals by chemical

analysis of CIPW (Cross, Iddings, Pirsson, and Washington). The mineral content of rock samples can be seen in table 3 and fig. 9. The highest percentage of olivine is in trachybasalt STA 19 (18,43 wt%), olivine is present only in basalt, gabbro, basaltic trachyandesite, and trachybasalt. Quartz is present only in basaltic andesite, andesite, trachyandesite and dacite, with highest percentage in dacite STA 2. Based on normative anorthite and albite percentage, plagioclase type can be distinguished: labradorite (STA 7, STA 8, STA 17, STA 20), andesine (STA 2, STA 14, STA 19, STA 27, STA 28) and oligoclase (STA 10). Diopside, a Ca-Mg clinopyroxene is present in all rock samples, the highest percentage is in andesite STA 7 (13,44 wt%).

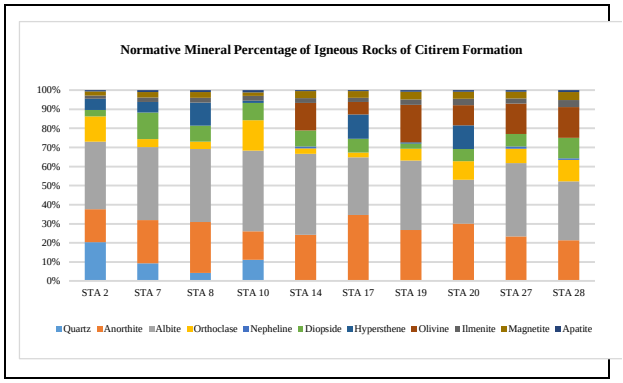

Fig. 9. Summary of Normative Minerals Percentage of Igneous Rocks of Citirem Formation

Hypersthene, an Mg-Fe orthopyroxene is absence in gabbro STA 14, basaltic trachyandesite STA 27 and trachybasalt STA 28, the highest percentage is in gabbro STA 17. Orthopyroxene is a Ca-poor pyroxene but rich in Fe and/or Mg, while clinopyroxene is rich in Ca and can contain Fe or Mg (Klein & Hurlbut, 1985). Orthopyroxene is commonly present in plutonic rocks. Orthopyroxene can be found in ultrabasic volcanic rocks, such as those found in basalt resulting from hotspot volcanic activity with tholeiitic magma type and in mid-ocean ridge basalt (MORB) forming an ophitic texture (Mulyaningsih, 2018). The presence of nepheline is only in gabbro STA 14 (0,98 wt%), basaltic trachyandesite STA 27 (1,15 wt%) and trachybasalt STA 28 (0,83 wt%). Orthoclase is presence in all samples, the highest percentage is in dacite STA 2 (13,18 wt%).

Based on plots of $Na_2O + K_2O$ vs SiO_2 volcanic rocks diagram (Middlemost, 1994), lithology can be distinguished: STA 2 is dacite, STA 7 is andesite, STA 8 is basaltic andesite, STA 10 is trachyandesite, STA 19 and 28 are trachybasalt, STA 20 is basalt, STA 27 is basaltic trachy-andesite (fig. 10A). While based on plots of TAS plutonic rocks diagram (Cox et al., 1979), STA 14 and STA 17 are gabbro, this is following the petrographic data (Fig. 10B).

Based on plot of K_2O vs SiO_2 (Peccerillo and Taylor, 1976) in fig. 11, it shows that the magma series of igneous rocks of Citirem Formation are divided into low-K (STA 7, STA 8), medium-K (STA 14, STA 17, STA 19, STA 27, STA 2), high-K (STA 10) and shoshonite (STA 20, STA 28).

The Ti element is considered stable and, therefore, has a high reputation for aiding the interpretation of petrogenesis. Therefore, even the TiO_2 values of basalt and basaltic andesite can determine whether the rock has an orogenic genesis or not. Trachybasalt (STA 19 and 28) and basalt (STA 20) have a TiO_2 content of > 1.3%, indicating that the basalts come from a non-orogenous environment. In comparison, the TiO_2 content of < 1.3% in basaltic andesite (STA 7 and 8) indicates that the rock formed in the orogen environment (Gill, 1981).

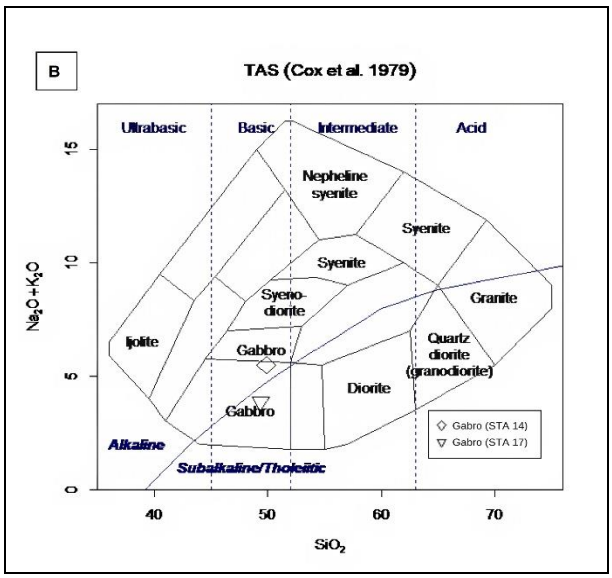

Fig. 10. A: The plots of the Citirem Formation rock samples and comparison rocks from Mirdita Ophiolite on the volcanic rocks TAS diagram (Middlemost, 1994) show that STA 2 is dacite, STA 7 is andesite, STA 8 is basaltic andesite, STA 10 is trachyandesite, STA 19 and 28 are trachybasalt, STA is 20 basalt, STA 27 is basaltic trachyandesite; B: The plot on the plutonic rocks TAS diagram (Cox et al., 1979), show that STA 14 and 17 are gabbro. The symbol of Citirem Formation rock samples are black.

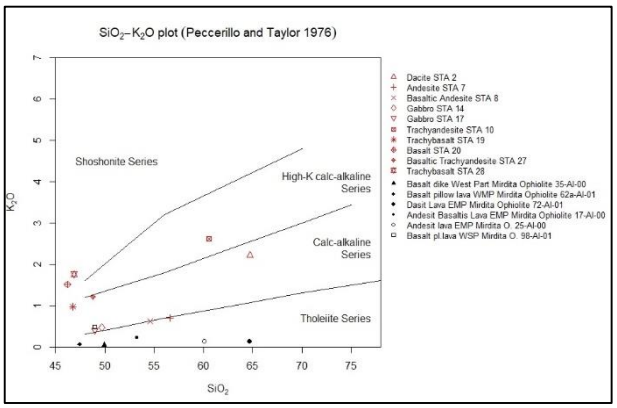

Fig. 11. Plots of Citirem Formation rock samples (research) and comparison rocks from Mirdita Ophiolite on K_2O vs SiO_2 diagram (Peccerillo and Taylor, 1976).

4.3.2 Geochemistry of Trace Elements

The potential for stability problems of the concentration of the major element during low-temperature hydrous metamorphism has been known for a long time. Therefore, most geochemical studies of underwater volcanic rocks on ophiolites are focused on the trace elemental composition of basaltic rocks, which carry the most stable information regarding magma sources and, by conclusion, tectonic environments (Metcalf &; Shervais, 2008). Incompatible elements in igneous rocks are particularly useful when investigating the active role of the crust and mantle in the genesis of magma (Thompson et al., 2014).

Analysis of trace elements in 10 rock samples is presented in table 4 (Rare Earth Elements) and table 5 (Non-Rare Earth Elements). High Ni, Cr, Co values (Ni = 250 – 300 ppm, Cr = 500 – 600 ppm) indicate that the element is a good indicator of knowing that the rock comes from the

derivation of parent magma sourced from the peridotite mantle (Wilson, 1989). In table 5, it is known that the elements Ni (9 – 157 ppm), Cr (6 – 222 ppm), and Co (10 – 37 ppm) have low levels and out of criteria. It shows that the Citirem Formation study rock samples are not a direct derivative of the parent magma sourced in the peridotite mantle.

Data on trace element content in the Citirem Formation rock samples are plotted on Th-Hf-Ta-Zr-Nb discriminant diagram (Wood, 1980), which can be seen in Fig. 12. Data were also primitive mantle long and NMORB-normalized (Sun and McDonough, 1989) are presented in the spidergrams in fig. 13.

Based on Th-Hf-Ta-Zr-Nb discriminant diagram, it is known that dacite STA 2, andesite STA 7, andesite basaltic STA 8, trachyandesite STA 10, and gabbro STA 14 are calc-alkaline basalt. Gabbro STA 17 indicates IAT (island arc tholeiitic). Trachybasalt STA 19, basalt STA 20, and basaltic trachyandesite STA 27 are E-MORB, WPT (within plate tholeiitic), while trachybasalt STA 28 is WPA (within-plate alkali).

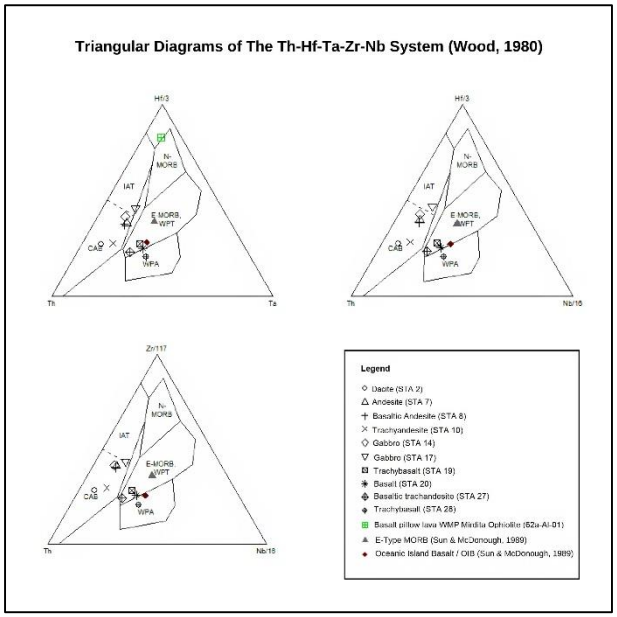

Fig. 12. Results of the Citirem Formation rock sample plot (research) and comparison rocks on the Th-Hf-Ta-Zr-Nb diagram (Wood, 1980).

Alkaline basalt and its derivatives are commonly found in intra-plate tectonic settings such as oceanic island basalts (OIB) and intracontinental plate expansions. Alkaline is rare but can also be found in tectonic environments related to subduction. Oceanic island basalts exhibit considerable diversity in composition, ranging from tholeiitic (Hawaii, Iceland, and Galapagos) to sodic-alkali (Canary Islands and St. Helena) to potassium-alkali (Tristan da Cunha and Gough) (Wilson, 1989). On oceanic islands, the co-existence of basalt tholeiite and alkali is found, and since Powers (1935), studied extensively in the Hawaiian archipelago. Macdonald and Katsura (1964) stated that a complete chemical gradation from tholeiitic to alkaline basalt does exist and that both types are layered on top of each other in a thin transition zone. Two magma suites evolved through fractional crystallization. Chen et al. (1991) and Frey et al. (1991) argue that the transition between tholeiitic and alkaline basalt can be associated with the early stages of caldera formation. Based on this information, it can be interpreted that the presence of trachy-basalt STA 28 which is a within-plate alkali is likely a co-existence with trachy-basalt STA 19, Basalt STA 20, and basaltic trachy-andesite STA 27, which is an E-MORB, within-plate tholeiitic.

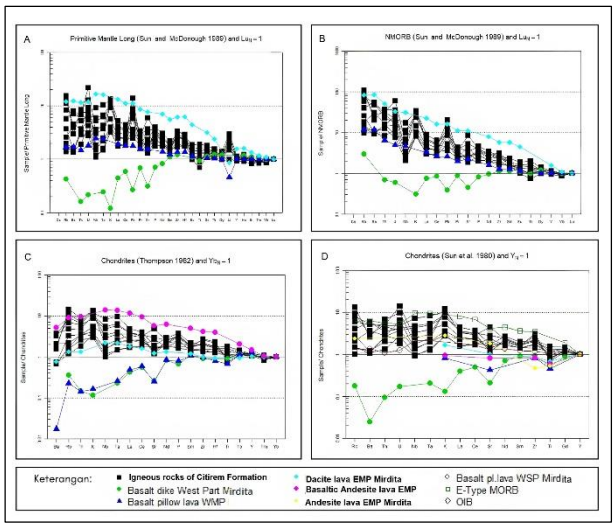

Fig. 13. Multielement spidergrams of Citirem Formation rock samples (A) primitive mantle long-normalized (Sun & McDonough, 1989), (B) NMORB-normalized (Sun & McDonough, 1989), (C) Chondrites-normalized (Thompson, 1982), (D) Chondrites-normalized (Sun et al., 1980).

Based on the spidergrams with primitive mantle long-normalized (Sun & McDonough, 1989) in Fig.13A and NMORB-normalized (Sun & McDonough, 1989) in Fig.13B, some patterns of trace elements of the Citirem Formation rock samples similar to Mirdita Ophiolites in Albania, namely with EMP (Eastern Main Profile) dacite lava which is predominantly SSZ (suprasubduction zone) affinity and some patterns also similar with WMP (Western Main Profile) basalt pillow lava which is predominantly affinity MORB. Even so, the pattern of trace elements of the Citirem Formation rock sample shows no resemblance to the western Mirdita Ophiolite basalt dike. Based on the spidergrams with chondrites-normalized (Thompson, 1982) in Fig. 13C, in general, the rock samples of the Citirem Formation have similar patterns with dacite lava and EMP basaltic andesite lava (Eastern Main Profile) of Mirdita Ophiolite. While the spidergrams with chondrites-normalized (Sun et al., 1980) in Fig. 13D show that some patterns of trace elements of the Citirem Formation rock sample have similarities with OIB (Oceanic Island Basalt), E-MORB (Enriched Mid Ocean Ridge Basalts), and also the andesite lava of SSZ EMP Mirdita Ophiolite. However, the rocks of the Citirem Formation are relatively enriched in elements U, K, Pb.

Oceanic-island basalt/OIB is systematically enriched in more incompatible trace elements. OIBs are ascribed to mantle sources enriched with deeper trace elements, and they may reflect complex multicomponent sources that include oceanic lithospheres recycled into the mantle through subduction. On average, E-MORB is enriched relative to N-MORB but to a lesser extent than OIB (Metcalf and Shervais, 2008). In comparison, the characteristic composition of basaltic magma of suprasubduction zones is an increase in the concentration of light ionic lithophile elements (LILE: Cs, Rb, Ba, Th, K, Sr, Pb) relative to high field strength elements (HFSE: Nb, Ta, Hf, Zr, Ti) (Wood, 1980; Saunders et al., 1980; Pearce, 1982; Pearce et al., 1984;

Metcalf and Shervais, 2008). LILE is highly soluble in water whereas HFSE is not. The enrichment of LILE compared to HFSEs in the magma thus indicates a source region enriched by an aqueous solution. The abundance of the most non-conservative elements (e.g., Cs, Ba, K, Pb, Th, U, P, La) suggests that the mantle source from which lava is produced has been enriched with these elements subduction. It indicates that the magma comes from enriched mantle sources (Dilek et al., 2008).

5. Discussion

Magmatism in modern oceanic basins can be considered representative of four main types: normal mid-ocean-ridge basalts (N-MORB), enriched mid-ocean-ridge basalts (E-MORB), within-plate or ocean-island basalts (OIB), and magmas of supra subduction zones. Basalt compositions dominate the N-MORB, E-MORB, and OIB suites; in contrast, suprasubduction zone suites have more diverse compositions, ranging from basalt compositions to more evolved compositions and their plutonic equivalents (Metcalf and Shervais, 2008).

Two possible scenarios can be proposed on the geochemical analysis of the Citirem Formation rock samples. First, all Citirem Formation rock samples are part of the suprasubduction zone system, so rock samples with E-MORB, WPT, and WPA affinities (STA 19, STA 20, STA 27, and ST 28) are rifting products when the slab undergoes rollback. Second, that rock samples with E-MORB, WPT, and WPA affinities (STA 19, STA 20, STA 27 and ST 28) are separate from the suprasubduction zone system as illustrated in Fig. 14 and may be Cretaceous in age as classically proposed by Sukamto (1975).

The SSZ oceanic crust formation's specific tectonic settings include the forearc, back arc, and incipient arc. Backarc tectonic settings may evolve as trench-proximal or distal trench-distal dispersal centers that exhibit the influence of subduction variables (Dilek and Furnes, 2011). Extrusive rocks and dike forearc ophiolites likely show progressive compositional and geochemical variations in time from MORB-like, then to IAT, then to the youngest boninite (Dilek et al.2008, Dilek and Thy 2009; Ishizuka et al. 2014). Based on the possible scenarios proposed, the sequence from old to young may be interpreted from E-MORB, within plate tholeiitic (WPT) basalt STA 20, trachy-basalt STA 19 and basaltic trachyandesite 27, and within plate alkali (WPA) trachybasalt STA 28, then island arc tholeiitic (IAT) gabbro STA 17, then to calc-alkaline gabbro STA 14, basaltic andesite STA 8, trachyandesite STA 10, andesite STA 7, and dacite STA 2. Even so, high Mg andesite with boninite affinity has not been found in this study.

However, It is necessary to do a dating method to determine the age of the Citirem Formation rocks from each magma affinity, whether or not it is the same as the basalt pillow lava of Gunung Badak, which is predominantly island arc calc - alkaline basalts with the origin of magma from tectonics related to subduction (Haq, 2017). Hardiyono, et al. (2023) published that age determination using radiometric K-Ar shows that Gunung Badak basalt pillow lava is 22.4 million years old (Early Miocene) and contradicts with previous publication that said that the lavas considered to have come from a MOR of Indian oceanic plate, Mesozoic in age, which was emplaced due to subduction in the Late Cretaceous (Thayyib et al., 1977). Sukamto (1975) mapped and reported that the lava was part of the Mesozoic Citirem Formation (Mcv). Differently, Rosana et al. (2019) reinterpreted that Gunung Badak pillowed lava as part of Jampang Volcanism and proposed to exclude the lava from the Ciletuh ophiolite complex (Satyana, 2021).

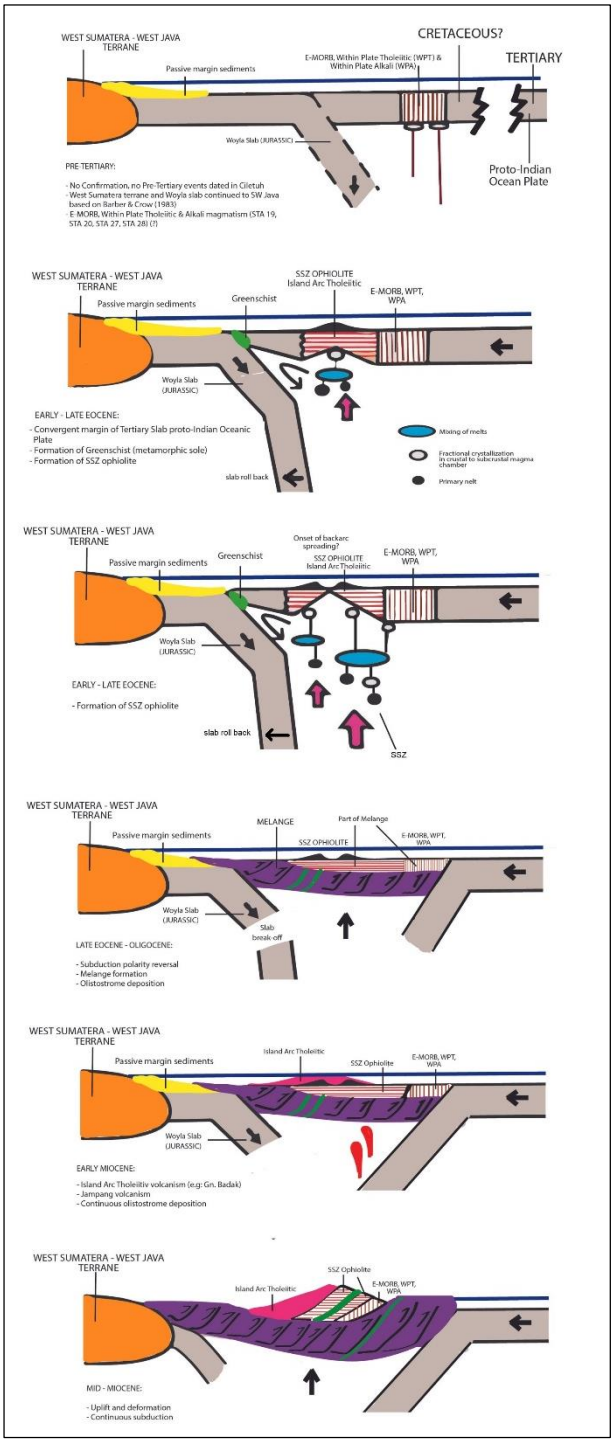

Fig.14. Illustration of possible scenarios of the magmatism development of the Citirem Formation (research) on the schematic sections of the Ciletuh tectonic evolution, in case the rock samples STA 19, STA 20, STA 27 and STA 28 (E-MORB, WPT and WPA affinities) are separate from the suprasubduction zone system (adapted from Dilek et al., 2008 and Satyana et al., 2021).

Based on the study's result, the Citirem Formation's rock samples have similarities in the variety of rocks, magma affinities and trace element patterns with SSZ and MORB Mirdita Ophiolite affinities. Suprasubduction zone ophiolites (SSZs) represent oceanic lithospheres formed on the extended upper plate of the subduction zone, analogous to modern Mirdita, Izu-Bonin-Mariana, and Tonga-

Kermadec arc-trench rollback systems (Stern and Bloomer 1992; Ishizuka et al. 2014; Pearce 2014). Subduction tectonic zones are an important to incorporating pre-existing oceanic lithospheres to continental margins. The oceanic lithosphere in the supra subduction zone ophiolites is part of the upper plate subduction system, but is over at the edge of the continent on the plate that descends through the collision process. This emplacement mechanism is through accretion, subduction, and collision processes. Among several popular mechanisms is the arc-continent collision caused by subduction polarity reversal or transference in the initiation episode of plate tectonic subduction (Yang, 2022).

The recommendation to follow up this study is the radiometric K-Ar dating method to determine the age of rocks, the sequence of magmatism, and grouping rocks by age. Sm-Nd isotope data is needed to provide better information on the magma source.

6. Conclusions

The igneous rocks of the Citirem Formation are petrographically composed of basalt, gabbro, andesite, and dacite. Based on plot of $Na_2O + K_2O$ vs SiO_2 diagram, specific lithology of rock samples was obtained: basalt, trachybasalt, basaltic trachyandesite, trachyandesite, andesite, dacite (Middlemost, 1994) and gabbro (Cox et al., 1979). Based on plot of K_2O vs SiO_2 (Peccerillo and Taylor, 1976), the magma series of igneous rocks of Citirem Formation are divided into low-K (STA 7, STA 8), medium-K (STA 14, STA 17, STA 19, STA 27, STA 2), high-K (STA 10) and shoshonite (STA 20, STA 28). Based on the plots of Th-Hf-Ta-Zr-Nb discriminant diagram (Wood, 1980), dacite STA 2, andesite STA 7, basaltic andesite STA 8, trachyandesite STA 10 and gabbro STA 14 are calc-alkaline. Gabbro STA 17 is island arc tholeiitic. Trachy-basalt STA 19, basalt STA 20 and basaltic trachyandesite STA 27 are E-MORB, WPT (within plate tholeiitic), while trachybasalt STA 28 is WPA (within plate alkali). Spidergrams with primitive mantle long – normalized, NMORB - normalized (Sun and McDonough, 1989) and chondrites - normalized (Sun et al., 1980 and Thompson et al., 1982) show distinctive patterns that have similarities with suprasubduction zone and MORB of Mirdita Ophiolite. But some patterns also show similarities with OIB and E-MORB (Sun and McDonough, 1989).

Acknowledgements

The author would like to thank Universitas Padjadjaran for funding this research through the Academic Leadership Grand (ALG) research scheme, to the Ciletuh-Palabuhanratu UNESCO Global Geopark Management Agency, as well as all colleagues who have helped the fieldwork process and research studio.

References

Dilek Y, Furnes H., 2011. Ophiolite genesis and global tectonics: Geochemical and tectonic fingerprinting of ancient oceanic lithosphere. Geological Society of America Bulletin 123: 387-411

Dilek Y, Furnes H, Shallo M., 2008. Geochemistry of the Jurassic Mirdita Ophiolite (Albania) and the MORB to SSZ evolution of a marginal basin oceanic crust. Lithos 100: 174-209.

Dilek Y, Thy P., 2009. Island arc tholeiite to boninitic melt evolution of the Cretaceous Kizildag (Turkey) ophiolite: Model for multi-stage early arc–forearc magmatism in Tethyan subduction factories. Lithos 113: 68-87

Gill, 1981. Orogenic andesites and Plate Tectonics. Volume 16, Minerals and Rocks. Berlin, Heidelberg, New York: Springer Verlag.

Haq, Hafidhah N., 2017. Petrologi Basalt Daerah Mandrajaya, Kecamatan Ciemas, Kabupaten Sukabumi, Provinsi Jawa Barat. SKRIPSI: Studi Petrologi Fakultas Teknik Geologi Universitas Padjadjaran.

Hardiyono, Adi, at al., 2023. New Consideration of Origin of The Gunung Badak Basaltic Lava, Ciletuh Area, Indonesia. Journal of Engineering Science and Technology Special Issue on AASEC2022. August (2022) 1-7. School of Engineering, Taylor's University.

Ishizuka O, Tani K, Reagan MK., 2014. Izu-Bonin-Mariana forearc crust as a modern ophiolite analogue. Elements 10: 115-120

Klein, C., and Hurlbut, C.S., Jr., 1985. Manual of Mineralogy, Wiley, 20th ed., p.476 ISBN 0-471-80580-7

Metcalf R.V. dan Shervais, John W., 2008. Suprasubduction-zone ophiolites: Is there really an ophiolite conundrum? The Geological Society of America Special Paper 438 USA.

Middlemost, Eric A.K., 1994. Naming materials in the magma/igneousrock system. Earth Science Reviews, 37, 215-244.

Mulyaningsih, Sri., 2018. Kristalografi dan Mineralogi Edisi 1 2018. Yogyakarta: Akprind Press.

Pearce, J.A., 1982. Trace element characteristics of lavas from destructive plate boundaries, in Thorpe, R.S., ed., Andesites: Orogenic Andesites and Related Rocks: Chichester, UK, John Wiley & Sons, p.525–548.

Pearce, J.A., Lippard, S.J., and Roberts, S., 1984. Characteristics and tectonic significance of supra-subduction zone ophiolites, in Kokelaar, B.P., and Howells, M.F., eds., Marginal Basin Geology: Palo Alto, California, Blackwell Scientific Publications, p. 74–94.

Pearce JA., 2014. Immobile element fingerprinting of ophiolites. Elements 10: 101-108

Rosana, M. F. 2006. Geologi Kawasan Ciletuh Sukabumi: Karakteristik, Keunikan, dan Implikasinya. Bandung: Universitas Padjadjaran.

Rosana, M.F., Isnaniawardhani, V., Hardiyono, A., Helmi, F., Brilian, C.H., Nugraha, K.S.A., Saragih, K.D., Ardiansyah, N., Ikhram, R., Zulfaris, D.Y., Agustin, F., Faturrakhman. M.L. 2019, Geological Map of the Cikadal-Lengkong Sheet (1208-43 and 1208-64 map sheets), University of Padjadjaran and Geological Survey of Indonesia.

Sartono, S., dan Murwanto, H., 1987. Olitostrom sebagai batuan dasar di Jawa. proseding PIT XVI IAGI, 19.

Satyana, A.H., 2021. Ciletuh Subduction, Southwest Java – New Findings: Nature, Age, and Regional Implications. Proceedings of the Indonesian Petroleum Association, 45th Annual Convention and Exhibition.

Saunders, A.D., Tarney, J., Marsh, N.G., and Wood, D.A., 1980. Ophiolites as ocean crust or marginal basin crust; a geochemical approach, in Ophiolites: Proceedings of the International Ophiolite Symposium: Cyprus, Nicosia, p. 193–204.

Schiller, D.M., Garrard, R.A., Prasetyo Ludi., 1991. Eocene Submarine fan sedimentation in Southwest Java. Proceedings IPA ke 20, Jakarta.

Stern RJ, Bloomer SH., 1992. Subduction zone infancy: Examples from the Eocene Izu-Bonin-Mariana and Jurassic California arcs. GSA Bulletin 104: 1621-1636.
Streckeisen. A.L., 1976. "To Each Plutonic Rock Its Proper Name," Earth Science Reviews, vol. 12, hal. 1–33.
Streckeisen, A. L., 1978. IUGS Subcommission on the Systematics of Igneous Rocks. Classification and Nomenclature of Volcanic Rocks, Lamprophyres, Carbonatites and Melilite Rocks. Recommendations and Suggestions. Neues Jahrbuch für Mineralogie, Abhandlungen, Vol. 141, 1-14.
Suhaeli, E.T., et al., 1977. The status of the melange complex in Ciletuh area, Southwest Java. Proceeding Indonesia Petroleum Assoc., 6th annual conv., hal 241-253.
Sukamto, Rab, 1975: Geologi Lembar Jampang dan Balekambang, Skala 1:100.000. Direktorat Geologi Bandung.
Sun S.S. dan McDonough W. F., 1989. Chemical and isotopic systematics of oceanic basalts: implication for mantle compotition and processes. Geol Soc. London. Spec. Pub. 42, pp. 313-345.
Thayyib, E.S., Said, E.L., Siswoyo, and Priyomarsono, S., 1977, The status of the melange complex in the Ciletuh area, South West Java, Proceedings Indonesian Petroleum Association, 6th Annual Convention, Jakarta, 241-254.
Thompson, R.N., et al., 2014. An Assessment of the Relative Roles of Crust and Mantle in Magma Genesis: An Elemental Approach (and Discussion). Philosophical Transactions of the Royal Society of London. Series A, Mathematical and Physical Sciences, Vol. 310, No. 1514, The Relative Contributions of Mantle, Oceanic Crust and Continental Crust to Magma Genesis (Apr. 27, 1984), pp. 549-590
Wood, D.A., 1980. The application of a Th-Hf-Ta diagram to problems of tectonomagmatic classification and to establishing the nature of crustal contamination of basaltic lavas of the British Tertiary volcanic province: Earth and Planetary Science Letters, v. 50, no. 1, p. 11–30, doi: 10.1016/0012-821X(80)90116-8.
Yang, Gaoxe., 2022. Subdution initiation triggered by collision: A review based on examples and models: Elsevier, Earth - Science Reviews, v. 232, September 2022, 104129, doi: 10.1016/j.earscirev.2022.104129